

3-5 Compact Clocks Using a Thin Cesium Cell

FUKUDA Kyoya, KINOSHITA Moto, HASEGAWA Atsushi, TACHIKAWA Maki,
and HOSOKAWA Mizuhiko

We study the effect of cell geometry on the electromagnetically induced transparency (EIT) spectrum using a thin Cs vapor cell as a first step for developing a compact frequency standard. When the cell thickness is less than 1 mm and the coupling radiation is sufficiently weak, the wall-to-wall transit time broadening is largely suppressed because only slow atoms have enough time to settle down on the dark state and contribute to the EIT signals. The observation of EIT spectrum reveals that a thin cell has the velocity selectivity caused by wall collisions.

Keywords

Electromagnetically induced transparency, Frequency reference, Thin cell, Velocity selectivity

1 Introduction

In recent years, laser spectroscopy employing a thin cell has attracted attention for its potential application to compact frequency standards [1]-[4], due to the technology's simple system configuration and extremely high resolution. In particular, spectral observation of the Cs atom in a thin cell will prove of vital importance in potential applications to compact atomic clocks and to frequency standards. This is because the Cs atom is at the heart of the definition of a second set forth in 1967 by the General Conference on Weights and Measures, or CGPM ("The second is the duration of 9,192,631,770 periods of the radiation corresponding to the transition between the two hyperfine levels of the ground state of an atom of Cs¹³³").

Intense research has been conducted relating to compact atomic clocks (CPT clocks) that employ quantum interference effects such as coherent population trapping (CPT) and electromagnetically induced transparency (EIT)[5] [6]. In a thin cell, only atoms having small velocity components perpendicular to the cell wall have sufficient opportunity to display coherent interaction with laser light.

Such velocity selectivity by the cell form also affects sharp three-level Λ -type resonance caused by the EIT phenomenon.

In research activities centering on frequency standards and frequency stabilization, studies relating to resolution of the spectral linewidth are indispensable. Therefore, as the first step in the development of a compact frequency standard, we investigated the dependence of the EIT spectrum on the cell form using a thin cell in which Cs vapor was enclosed. Experimental conditions relating to the thickness of the cell, laser intensity, and so on are important parameters within such an experimental system. If future application to compact atomic clocks is the goal, this experiment will, we believe, prove highly useful.

We observed the EIT signal that corresponded to the CPT of the ground states ($F = 3, m_F = 0$) and ($F = 4, m_F = 0$). The signal linewidth was measured as a function of laser intensity and cell thickness. Our experiment was conducted using glass cells with thicknesses of 0.3 mm, 1 mm, and 40 mm in which Cs vapor was enclosed. When the cell thickness was 1 mm or less and the laser intensity was sufficiently weak, transit time broadening between the cell walls was greatly reduced.

2 Geometric effect due to thin cell

Since the mechanisms of CPT and EIT phenomena have been discussed in a variety of previous reports[7], here we will forego a detailed description of these mechanisms.

In the representation of the uncertainty principle between energy and time ($\Delta E \cdot \Delta t \geq \hbar$, where ΔE and Δt are the uncertainties of energy and of time respectively, \hbar is Plank's constant), substituting ΔE with $2\pi\hbar \cdot \Delta\nu$ ($\Delta\nu$: linewidth), the EIT spectral linewidth of light transmitted from the atom in a thin cell is described by

$$\Delta\nu \geq \frac{1}{2\pi \cdot \Delta t} \quad (1)$$

which indicates that the spectral linewidth is inversely related to the uncertainty of time. Here, the uncertainty of time refers to the period in which the atom and the laser light are in coherent interaction with each other. As shown in Fig.1, consider an atom having a velocity component v_z perpendicular to the cell wall and an atom having a velocity component v_x parallel to the cell wall. If the cell thickness L and the laser diameter D are finite values, coherent interaction time is governed by the sum of the time in which the atom is relaxed by collision with the cell walls ($L/|v_z|$) and the time required for the atom to traverse beyond the diameter of the laser light ($D/|v_x|$). Here, it is assumed that the atom density in the cell is very small and that the effects of collision between the atoms can be ignored. Since

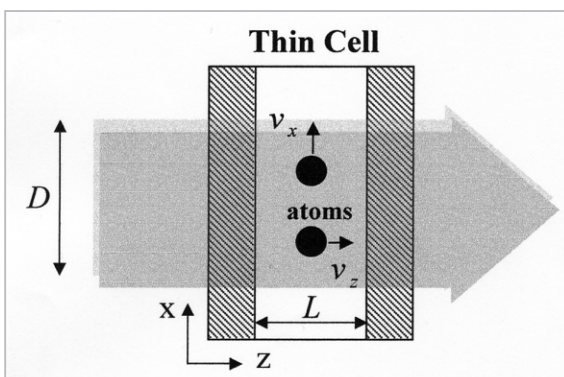


Fig.1 Atoms in a thin cell

the linewidth of the EIT signal is inversely related to the duration of the coherent interaction between the atom and laser, it can be concluded that with increasing thickness of the cell and diameter of the laser, the linewidth becomes narrower.

3 Experiment

Fig.2 shows the experimental setup designed to observe the EIT spectrum, and Fig.3 shows the energy levels of the Cs atom. We prepared a Cs vapor cell made of cylindrical Pyrex glass 3-mm thickness with a diameter of 34mm. The atom density of the Cs atom is about $3 \times 10^{10}/\text{cm}^3$ at room temperature. The mean free path for atomic collision sufficient to affect atomic velocity is approximately 1.4 m. The extended cavity diode laser (ECDL) is tuned to a transition of $S_{1/2}(F = 4) \rightarrow P_{3/2}(F' = 4)$ of the D_2 line of Cs atom. Output light is transmitted through a 9.19-GHz electro-optic modulator (EOM). An upper sideband of the spectrum of this transmitted light is used as probe light for the $F = 3$ state. Frequency spacing between the carrier and the sideband spectrum is provided by a stable microwave synthesizer. When this microwave frequency agrees with the hyperfine structure interval of the ground state, an almost Lorentzian absorption spectral profile is observed as a variation in transmitted light intensity. The spectrum is recorded by observing the transmitted light intensity as a function of the frequency of the synthesizer. The laser light has a diameter of approximately 14mm, which results in transit time broadening of approximately 2.4kHz for atoms traveling at mean velocity. The upper sideband contains about 15% of the original laser intensity, and about 70% remains in the carrier spectrum. In order to obtain the EIT signal, the laser light is focused on a high-sensitivity Si-pin photodiode after passing through the cell. The intensity of the laser light is amplitude-modulated by the synthesizer with a modulation frequency in the range of 50-300kHz. An output signal from the photodiode is lock-in detected at this modulation frequency.

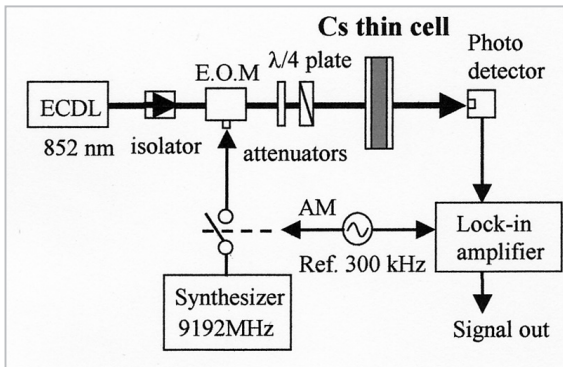


Fig.2 Schematic diagram of the experimental setup

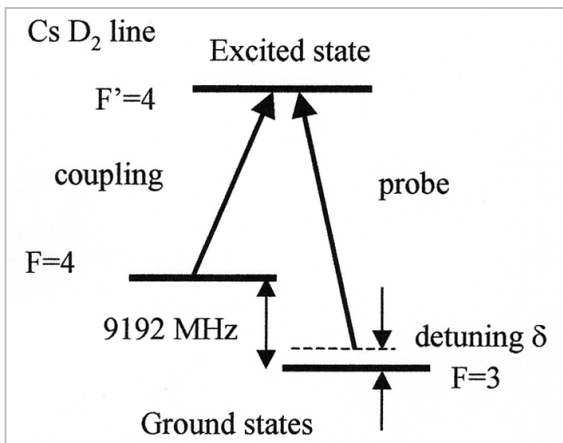


Fig.3 Energy diagram of Cs atom

4 Experimental results

Fig.4 shows a typical EIT signal observed according to the above-mentioned procedure. The vertical axis represents the transmitted light intensity, and its scale is given in arbitrary units (a.u.). The horizontal axis represents detuning of the probe light in units of MHz. The figure indicates that in the vicinity where the detuning of the probe light is zero, the signal intensity tends to increase. That is, in this region, the transmitted light intensity of the laser increases.

4.1 Zeeman splitting of EIT spectrum

Our glass cell is disposed in a single cylindrical magnetic shield. With this shield, the remaining magnetic field can be decreased to $1\mu\text{T}$ or less. Because this field cannot be reduced to zero due to the influence of geomagnetism and other external magnetic fields,

degeneration is resolved to hyperfine levels with slight energy differences, and multiple EIT spectra having different attributive conditions will overlap, with small frequency shifts in between. Therefore, measurement of the linewidth of the spectrum shown in Fig.4(a) does not give a correct value. Subsequently, by enclosing the cell with a solenoid coil to apply a magnetic field, we observed the seven-split spectra produced from the splitting of the magnetic sub-levels by the Zeeman effect. Here, the seven-split spectra are designated $(-3, -3)$, $(-2, -2)$, and so on from left

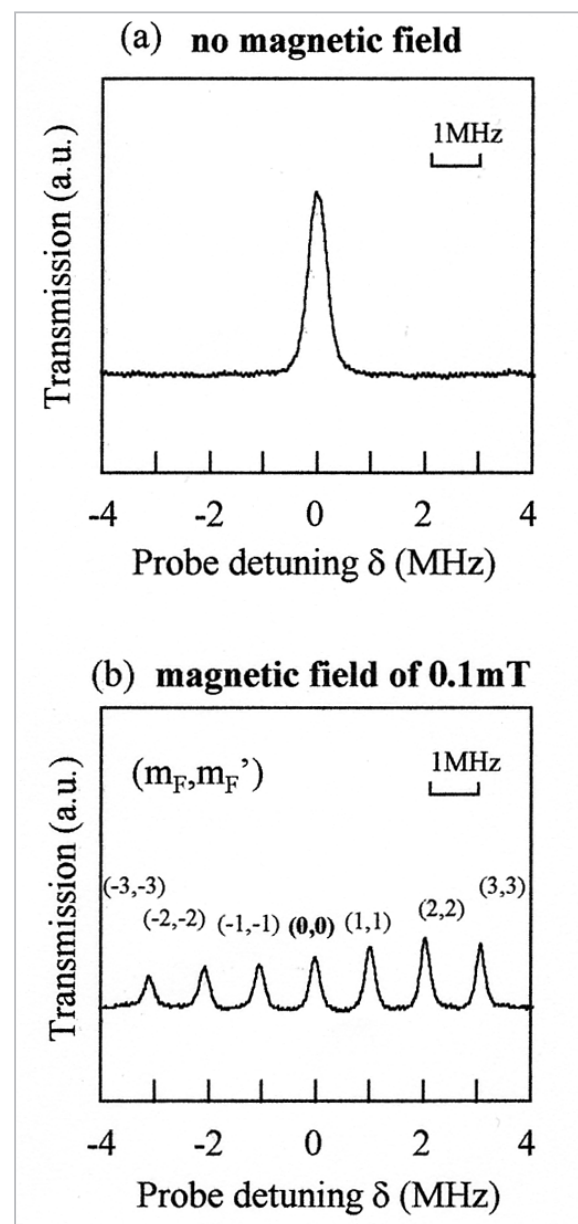


Fig.4 EIT spectrum of Cs atoms

to right, through (3, 3), since the spectra are connected with m_F of the $6S_{1/2}(F = 3)$ state and the $6S_{1/2}(F = 4)$ state; this connection contributes to the Λ type transition. The magnetic field is applied parallel to the laser irradiation

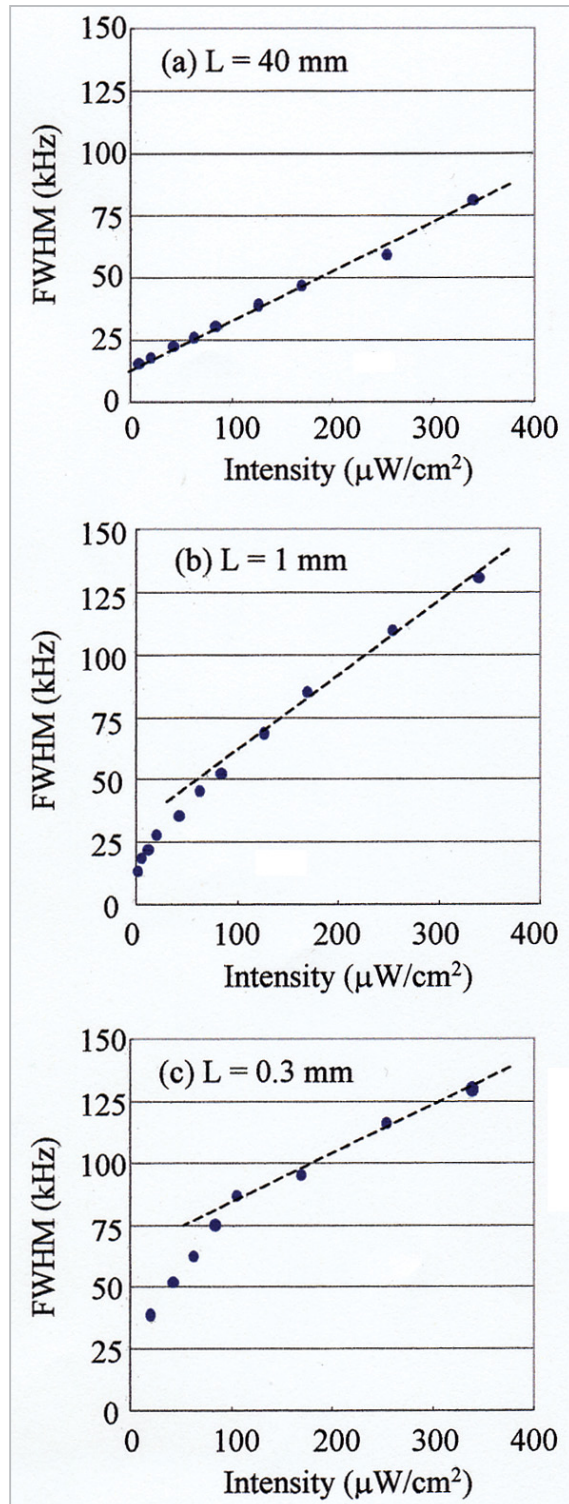


Fig.5 Dependence of the linewidth of the observed EIT spectrum on laser intensity

axis so that the laser is transformed into circular polarized light σ^+ that allows only a transition of $\Delta m_F = +1$; the magnitude of the applied field is 0.1 mT. The seven-split spectra are shown in Fig.4(b). Here we will discuss only the linewidth of the central signal peak (0,0) that corresponds to the coherence between two ground states ($F = 3, m_F = 0$) and ($F = 4, m_F = 0$).

4.2 Dependence of linewidth of EIT spectrum on laser intensity

The geometrical effect between the cell wall and the atom and the intensity of the laser light represent significant factors determining the linewidth of the EIT spectrum. Fig.5 shows the dependence of the linewidth of the EIT spectrum on the laser intensity with three glass cells of different thicknesses (40 mm, 1 mm, and 0.3 mm). When the cell thickness is 40 mm, the EIT linewidth increases linearly with respect to the laser intensity. In addition, when the thicknesses are 1 mm and 0.3 mm, the linewidths show linear tendencies relative to laser intensity in the region where the latter is comparatively intense. However, the linewidth shows a clearly different tendency in the region where the laser intensity is weak. This tendency is particularly remarkable with a thickness of 0.3 mm.

5 Considerations

5.1 Analysis of velocity distribution of non-coupled $INC >$ state by rate equation

The absorption spectral linewidth of a two-level atom broadens with increasing intensity of the irradiated laser light. This is because the Rabi frequency becomes large in proportion to the square root of the laser intensity, and consequently the transition time between the levels—i.e., the duration of interaction between the atom and the laser—becomes short. Moreover, if the laser intensity is weak, the linewidth increases in a nearly linear manner. This phenomenon is referred to as the power broadening effect.

This experiment is designed to treat a

three-level system and evaluate the transmitted light spectrum using the quantum interference effect caused by irradiation of two laser light beams; therefore, we cannot apply the above conclusions without modification. Nevertheless, Arimondo demonstrated in a report [6] that the linewidth of the EIT spectrum increases linearly with respect to the increase in laser intensity in the region where the laser intensity is weak (specifically, the range in which the laser intensity is one-tenth the saturation intensity or less). He explained this phenomenon by the saturation broadening law, obtained from density matrix analysis. Since the range of the laser intensity used for our signal observation was one-tenth the saturation intensity or less, it is believed that this saturation broadening law is applicable to the results of the present experiment. Therefore, it may be concluded that the phenomenon seen in our experimental results, in which the linewidth increases linearly with respect to the increase in the laser intensity, is attributable to the saturation broadening effect. In our experimental results, it turned out that the spectral linewidth observed for the atoms in the thin cell was narrower than the value predicted based on the saturation broadening effect and transit time broadening. This result will be discussed in more detail below.

As stated above, the linewidth of the EIT spectrum is inversely related to the interaction time between the atom and the laser light (when the laser intensity is not taken into consideration). Since the interaction time is essentially the time required for the atom to travel between the cell walls or the time required for the atom to traverse the diameter of the laser light, these linewidths will naturally depend on the atomic velocity. That is, because an atom having a low velocity interacts with the laser light for a longer period, the linewidth of the EIT spectrum of that atom becomes narrow. In contrast, because an atom at high velocity interacts more briefly with the laser light, the linewidth of the EIT spectrum of that atom becomes wide. Therefore, if atoms having low velocities contribute signifi-

cantly to the EIT signal, the linewidth should become narrower than the value calculated based on power broadening or cell thickness. We concluded that when the laser intensity was sufficiently weak, such a phenomenon occurred in the thin cell, and we obtained a velocity distribution of the atoms contributing to the EIT signal using a simple rate equation model. It is convenient to describe the evolution of the system in the basis of coupled $|C\rangle$ and non-coupled $|NC\rangle$ states [7]. The model (Fig.6) and the rate equation are shown below.

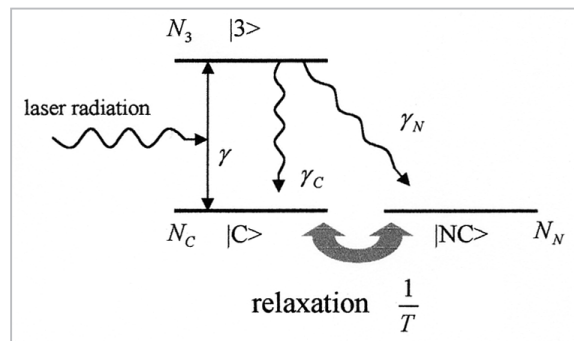


Fig.6 Rate equation model

Considering the model as described above, the rate equation can be expressed as

$$\begin{aligned} \frac{dN_C(v_z)}{dt} &= -\gamma(N_C(v_z) - N_3(v_z)) + \gamma_C N_3(v_z) - \frac{N_C(v_z) - N_C^*(v_z)}{T} \\ \frac{dN_N(v_z)}{dt} &= \gamma_N N_3(v_z) - \frac{N_N(v_z) - N_N^*(v_z)}{T} \\ \frac{dN_3(v_z)}{dt} &= \gamma(N_C(v_z) - N_3(v_z)) - (\gamma_C + \gamma_N)N_3(v_z) \end{aligned} \quad (2)$$

This equation incorporates: an optical pumping rate γ between $|C\rangle$ state and excited $|3\rangle$ state; relaxation rates γ_C and γ_N from $|3\rangle$ state to $|C\rangle$ state and $|NC\rangle$ state through spontaneous emission; and a relaxation effect between $|C\rangle$ state and $|NC\rangle$ state,

$$\frac{1}{T} = \frac{\bar{v}_x}{D} + \frac{|v_z|}{L} \quad (3)$$

The first term in equation (3) represents the relaxation effect of the atom travelling out of the diameter of the laser light, where \bar{v}_x denotes the most probable value of the atom's

velocity component parallel to the cell wall and D denotes the diameter of the laser light. The second term represents the relaxation effect due to collision of the atom with the cell walls, where $|v_z|$ denotes the absolute value of the atom's velocity component perpendicular to the cell walls and L denotes the distance between the cell walls (i.e., the cell thickness). The optical pumping rate γ is expressed by

$$\gamma = \frac{\Omega_P^2 \gamma_C + \Omega_N^2 \gamma_N}{\Gamma^2} \quad (4)$$

where Ω_p and Ω_c denote the Rabi frequencies of the probe light and of the coupling light, and Γ denotes the spontaneous emission rate of an excited state. $N_C(v_z)$, $N_N(v_z)$, and $N_3(v_z)$ denote velocity distributions; namely, the numbers of atoms with velocity component v_z perpendicular to the cell wall of $|C\rangle$ state, $|NC\rangle$ state, and $|3\rangle$ state, respectively. $N_C^*(v_z)$ and $N_N^*(v_z)$ denote distributions of velocity components perpendicular to the cell wall in various states, each in thermal equilibrium. Values except $N_C(v_z)$, $N_N(v_z)$, and $N_3(v_z)$ can be estimated roughly if the laser intensity, the cell thickness, room temperature, and the like are given. Then by substituting all of the variables on the left side of equation (2) (temporal variations of $N_C(v_z)$, $N_N(v_z)$, and $N_3(v_z)$) with zeros, one may obtain the solution for the steady state. Here, since we are considering the behavior of an ensemble of atoms rather than a single atom, and because the laser oscillates a continuous wave, we may conclude that this model will provide excellent approximation of experimental results. Fig.7 shows a velocity distribution of the atoms contributing to EIT $N_N(v_z)$. Here, distributions in the region where the laser intensity is weak are shown for different cell thicknesses. From the figure, we can conclude that in the case of the 40-mm cell, the distribution takes an almost Maxwell-Boltzmann velocity distribution, but in the case of other cells, with decreasing thickness of the cell, the percentage of slow atoms increases, which results in a non-Maxwell-Boltzmann distribution with a pointed peak.

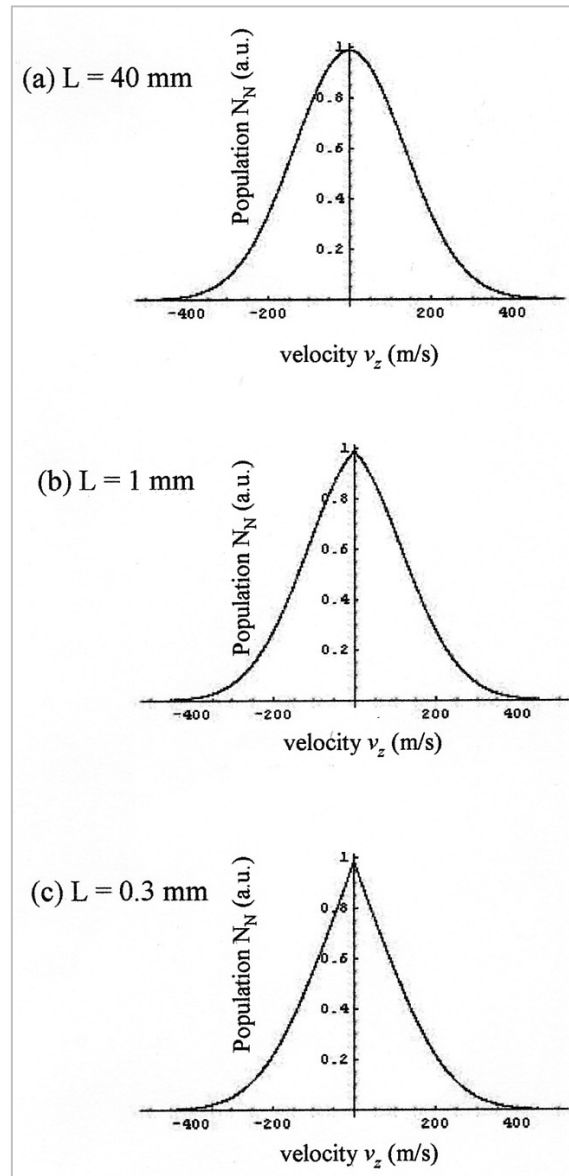


Fig.7 Velocity distribution of atoms in the non-coupled state

These observations can be understood as follows. It takes a finite time for the atom to settle into $|NC\rangle$ state after being irradiated by the laser. Since the transition process to $|NC\rangle$ state includes a transition by light, the time required for the atom to conduct this transition by light will be reduced if the laser light is intense and will lengthen if it is weak. Currently, we are considering a region in which laser intensity is weak; thus, the latter phenomenon will be observed. Atoms at high velocities will collide more quickly with the walls of the thin cell and will be phase-relaxed earlier than they will settle into $|NC\rangle$ state in

the region where the laser intensity is weak to some degree and will be unable to transmit to $|NC\rangle$ state. Consequently only atoms at low velocities will have sufficient time to interact with the light in the thin cell, consequently transitioning to $|NC\rangle$ state and contributing to the EIT signal. It is understood that this is the mechanism leading to the results shown in Fig.7.

5.2 Analysis of linewidth of EIT spectrum

Here, the EIT spectrum will be calculated from the velocity distribution of $|NC\rangle$ state obtained in the previous section. In this case we assume that by multiplying $N_N(v_z)$ with a weight $f(\delta)$ and integrating it for all velocities, we may obtain the transmitted light intensity α via the following equation,

$$\alpha \propto \int_{-\infty}^{\infty} f(\delta) N_N(v_z) dv_z \quad (5)$$

Here, $f(\delta)$ is expressed by

$$f(\delta) = \frac{1/T + \beta I}{\delta^2 + (1/T + \beta I)^2} \quad (6)$$

and is a Lorentzian function of detuning δ . We assume that this equation represents an EIT spectrum for a single atom. Character I denotes the laser intensity. β is introduced in the equation in consideration of the power broadening effect, and is referred to as the power broadening coefficient. Since this value cannot be calculated from the analysis of the rate equation, experimental results are introduced. We regarded the variation in the linewidth with respect to the laser intensity in the case of (a) $L = 40$ mm (Fig.5) as a straight line, and designated its slope as β . Then α was calculated as a function of detuning δ by substituting the equation (6) in the equation (5) and integrating it. A typical example of a region in which the laser intensity is weak as a result EIT spectrum is shown in Fig.8.

This figure shows that the 40-mm cell and the 0.3-mm cell yield different EIT spectral shapes. One can see that the EIT spectrum for the 0.3-mm cell has a steeper peak relative to

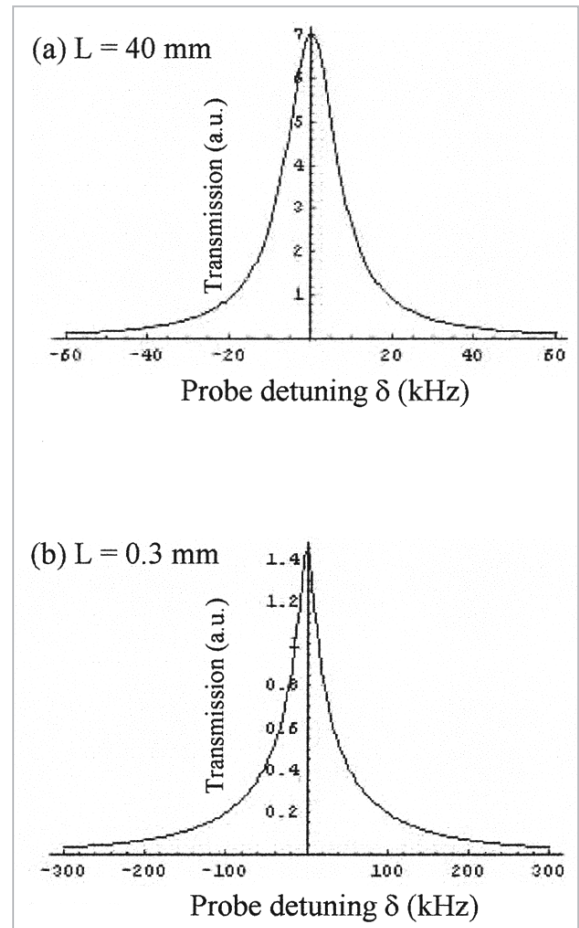


Fig.8 Calculated EIT spectrum

that for the 40-mm cell. If the spectrum takes such a shape, it is very likely that its linewidth will be narrower than calculated based only on power broadening and cell thickness. Fig.9 shows the dependence of the full width at half maximum of the EIT spectrum thus obtained on the laser intensity for different cell thicknesses.

The figure indicates that in the region of high laser intensity, variation in the dependence of linewidth on laser intensity itself displays a linear dependence on power broadening. However, in the region of weak laser intensity, the linewidth of the EIT spectrum is narrower than calculated based only on power broadening and cell thickness. Moreover, this phenomenon became more notable with thinner cells. Given the above, we came to the conclusion that this analysis of the linewidth of the EIT spectrum using the rate equation can reproduce the experimental values qualita-

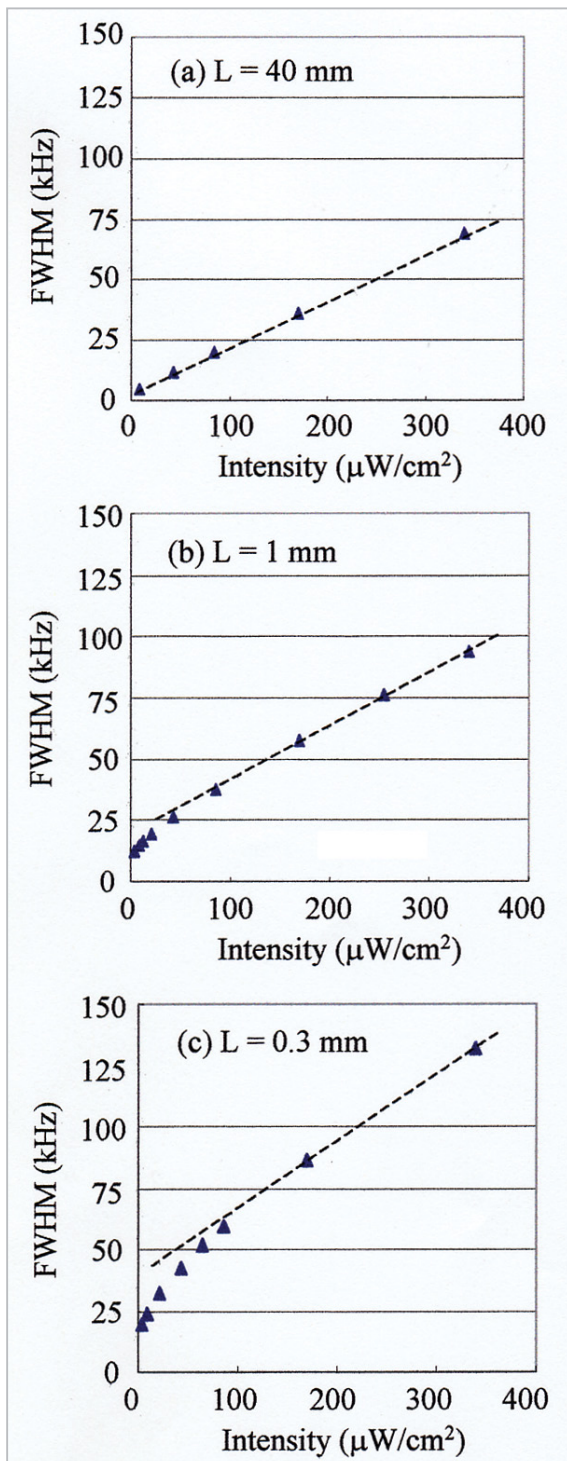


Fig.9 Dependence of the linewidth of the calculated EIT spectrum on the laser intensity

tively well.

Compact atomic clocks have previously been developed using the conventional optical-microwave double resonance method

[8][9]. These clocks employ a gas cell within a microwave resonator. Reduction in the size of such clocks has been restricted by the size of the microwave resonator. Today, however, the miniaturization of the atomic clock has become possible, through the use of all-optical pumping methods such as CPT and EIT.

Development of a compact atomic clock based on the CPT phenomenon was demonstrated by Kitching et al.[5]. They reported successful frequency stability of 1.3×10^{-10} for an integration time of 1 second using a glass cell with a thickness of 10 mm. The major drawback in using a thin cell, however, is that the signal-to-noise ratio (S/N) is restricted due to the short duration of interaction. In order to maintain velocity selectivity, it is necessary to maintain sufficiently low atomic vapor pressure in the cell. This may pose a significant problem in the use of a thin cell for a compact atomic clock. However, when the laser intensity is sufficiently weak in a thin cell, only those atoms having extremely low velocities will settle into the dark state, and consequently a very sharp spectrum can be easily obtained.

6 Conclusions

We have investigated the spectral profile of the EIT resonance of Cs atoms enclosed in a thin cell. The observed spectral linewidth of the atoms in the thin cell was narrower than the value calculated based on laser intensity broadening and transit time broadening. It is proposed that such spectral narrowing may be attributed to a non-Maxwellian velocity distribution caused by a balance between optical pumping and relaxation induced by the cell walls. The observation of the EIT spectrum has clearly shown that the thin cell features velocity selectivity. A more detailed analysis of the EIT spectrum of the atoms in the thin cell is currently being advanced using a density matrix[10].

References

- 1 A. Ch. Izmailov, Opt. Spectrosc. 74, 25, 1993.
- 2 S. Briaudeau et al., Phys. Rev. A 59, 3723, 1999 .
- 3 B. Zambon et al., Opt. Commun. 143, 308, 1997.
- 4 M. Tachikawa et al., Jpn. J. Appl. Phys. 37, L1559, 1998.
- 5 J. Kitching et al., Electron. Lett. 37, 1449, 2001.
- 6 C. Affolderbach et al., Appl. Phys. B 70, 407, 2000.
- 7 For example, E. Arimondo: Fundamentals of Quantum Optics 3, Lecture Notes in Physics, Vol. 420, 170, 1994.
- 8 P. J. Chantry et al., Proc. 1996 IEEE Int. Frequency Control Symp., 1002, 1996.
- 9 M. Bloch et al., Proc. 1993 IEEE Int. Frequency Control Symp., 164, 1993.
- 10 K. Fukuda et al., in preparation.



FUKUDA Kyoya

Senior Researcher, Atomic Frequency Standards Group, Applied Research and Standards Division

Frequency Standard, Laser Spectroscopy



HASEGAWA Atsushi, Ph. D.

Senior Researcher, Quantum Information Technology Group, Basic and Advanced Research Division

Non-linear Laser Spectroscopy



HOSOKAWA Mizuhiko, Ph. D.

Leader, Atomic Frequency Standards Group, Applied Research and Standards Division

Atomic Frequency Standards, Space Time Measurements

KINOSHITA Moto

Department of Physics, Meiji University

Quantum Electronics

TACHIKAWA Maki, Dr. Sci.

Associate Professor, Department of Physics, Meiji University

Quantum Electronics, Laser Spectroscopy

